

Rocking curve peak shift in thin semiconductor layers

C. R. Wie

Citation: *J. Appl. Phys.* **66**, 985 (1989); doi: 10.1063/1.343482

View online: <http://dx.doi.org/10.1063/1.343482>

View Table of Contents: <http://jap.aip.org/resource/1/JAPIAU/v66/i2>

Published by the [American Institute of Physics](#).

Related Articles

High Seebeck effects from conducting polymer: Poly(3,4-ethylenedioxythiophene):poly(styrenesulfonate) based thin-film device with hybrid metal/polymer/metal architecture
[APL: Org. Electron. Photonics 5, 238 \(2012\)](#)

High Seebeck effects from conducting polymer: Poly(3,4-ethylenedioxythiophene):poly(styrenesulfonate) based thin-film device with hybrid metal/polymer/metal architecture
[Appl. Phys. Lett. 101, 173304 \(2012\)](#)

Response to "Comment on 'Silver/silicon dioxide/silver sandwich films in the blue-to-red spectral regime with negative-real refractive index'" [*Appl. Phys. Lett.* 101, 156101 (2012)]
[Appl. Phys. Lett. 101, 156102 \(2012\)](#)

On the determination of the glass forming ability of $\text{Al}_x\text{Zr}_{1-x}$ alloys using molecular dynamics, Monte Carlo simulations, and classical thermodynamics
[J. Appl. Phys. 112, 073508 \(2012\)](#)

Enhanced photoanode properties of epitaxial Ti doped $\alpha\text{-Fe}_2\text{O}_3$ (0001) thin films
[Appl. Phys. Lett. 101, 133908 \(2012\)](#)

Additional information on J. Appl. Phys.

Journal Homepage: <http://jap.aip.org/>

Journal Information: http://jap.aip.org/about/about_the_journal

Top downloads: http://jap.aip.org/features/most_downloaded

Information for Authors: <http://jap.aip.org/authors>

ADVERTISEMENT



Special Topic Section:
PHYSICS OF CANCER

Why cancer? Why physics? [View Articles Now](#)

TABLE II. Demagnetizing factor in a uniformly magnetized cylinder N_z . a' is evaluated from Eq. (2b) and b' is evaluated from the exact expression given by Arrott *et al.* (Ref. 4). The percentage difference is $[(a' - b')/b'] \times 100$.

Dimensional ratio n	N_z		Percentage difference
	a'	b'	
0.1	0.815876	0.796677	2.41
0.2	0.689013	0.680175	1.30
0.3	0.596293	0.594731	0.26
0.5	0.469841	0.474490	-0.98
0.7	0.387637	0.393310	-1.44
1	0.307054	0.311577	-1.45
2	0.181372	0.181864	-0.27
3	0.128696	0.127769	0.73
5	0.081408	0.079907	1.88
7	0.059533	0.058086	2.49
10	0.042431	0.041193	3.01
12	0.035611	0.034501	3.22
15	0.028693	0.027739	3.44
20	0.021675	0.020908	3.67
30	0.014555	0.014008	3.91
50	0.008784	0.008438	4.10
70	0.006290	0.006038	4.19
100	0.004412	0.004232	4.25

Arrott *et al.*^{4,5} and Joseph.⁶ It is also found that the values of the demagnetizing factor of the cylinder, which are given in the text of Bozorth⁸ and are cited in many texts^{9,10}, are different from those estimated from the exact expression^{4,5,6} of the demagnetizing factor of the cylinder.

¹C. Kittel and J. Galt, in *Solid State Physics*, edited by F. Seitz and D. Turnbull (Academic, New York, 1956), Vol. 3, p. 502.

²P. Rhodes and G. Rawlands, Proc. Leeds Philos. Lit. Soc. Sci. Sect. 6, 191 (1954).

³W. F. Brown, Jr., *Magnetostatic Principles in Ferromagnetism* (North-Holland, Amsterdam, 1962). See the Appendix and Tables A1, A2, and A3.

⁴A. S. Arrott, B. Heinrich, T. L. Templeton, and A. Aharoni, J. Appl. Phys. 50, 2387 (1979).

⁵A. S. Arrott, B. Heinrich, and A. Aharoni, IEEE Trans. Magn. MAG-15, 1228 (1979).

⁶R. I. Joseph, J. Appl. Phys. 37, 4639 (1966).

⁷S. Middelhoek, J. Appl. Phys. 34, 1054 (1963).

⁸R. M. Bozorth, *Ferromagnetism* (Van Nostrand, Reinhold, New York, 1951), p. 845.

⁹S. Chikazumi, *Physics of Magnetism* (Wiley, New York, 1964), p. 19.

¹⁰K. Ohta, *Zikikohgaku no Kiso I* (Kyohritsu Shuppan, Tokyo, 1973), p. 38 (in Japanese).

Rocking curve peak shift in thin semiconductor layers

C. R. Wie

State University of New York at Buffalo, Department of Electrical and Computer Engineering, Bonner Hall, Amherst, New York 14260

(Received 20 February 1989; accepted for publication 5 April 1989)

A simple x-ray diffraction method for determining layer composition and mismatch is by measurement of the separation of peaks in a rocking curve. This method can only be used for layers with a thickness above a certain value. This minimum thickness can be significantly large for layers with a small lattice mismatch as in AlGaAs/GaAs or isoelectronic-doped III-V semiconductor layers. We give such an example and show that the interference between the diffraction amplitudes of the thin layer and that of the substrate is responsible for the peak shifting of the layer Bragg peak. When this peak shifting is significant, the kinematical diffraction theory and the peak separation method should not be used for the mismatch measurement, and only the dynamical diffraction theory simulation should be used. We present a criterion on the layer thickness, below which the dynamical theory simulation must be used. This thickness is inversely proportional to the lattice mismatch and does not depend on the diffraction geometry, wavelength, and substrate material.

Lattice mismatch and film composition of semiconductor heterojunction epitaxial layers are commonly measured by x-ray diffraction.¹⁻³ A quick and easy method is by measuring the separation of peaks in the rocking curve, from which the lattice mismatch and composition are calculated by considering the unit cell distortion and Vegard's law.⁴ Fewster and Curling⁵ showed a few examples of rocking curves for which the peak separation method is invalid due to the peak-shifting effect caused by the substrate or by other thicker layers. They did not, however, explain the exact cause of such peak shifting nor gave any criterion for what samples the peak separation method should not be used. Un-

derstanding the exact cause of the peak shifting is important for determining whether any approximation made in a diffraction model is valid or not.

Figure 1(a) shows the 004 $\text{CuK}\alpha_1$ rocking curves of a GaAs epitaxial layer doped with an isoelectronic dopant (In), grown on a GaAs(001) substrate by liquid phase epitaxy (LPE). The isoelectronic doping technique is used to improve III-V epitaxial layer quality by reducing the background dislocation and electron trap densities.⁶ The rocking curves in Fig. 1(a) are taken from an as-grown sample (curve a) and after successive 2-min chemical etching (curves b, c, and d). These curves have been reported in Ref.

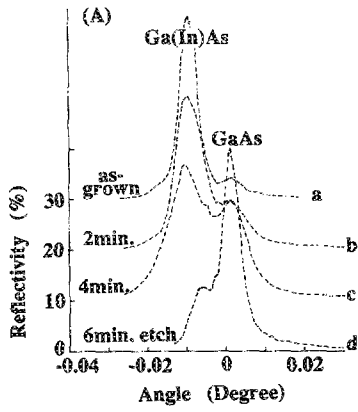
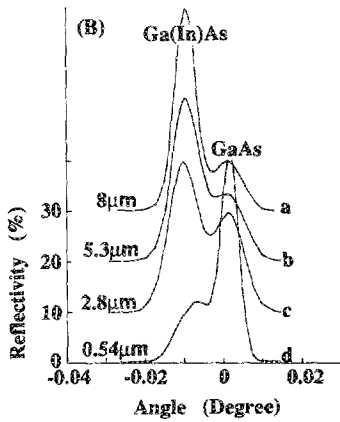


FIG. 1. (a) Experimental rocking curves of an indium-doped LPE GaAs layer on a GaAs substrate, taken after successive chemical etching. (b) Simulated rocking curves for different layer thicknesses.



7 and are reproduced here. In Fig. 1(b) we show the simulated rocking curves, calculated using the dynamical diffraction theory³ with a perpendicular x-ray strain of $0.028\% \pm 0.002\%$ which corresponds to the x value of $0.22\% \pm 0.016\%$ in the $\text{Ga}_{1-x}\text{In}_x\text{As}$ epilayer. The curves a, b, c, and d in Fig. 1(b) corresponds to the Ga(In)As layer thickness of 8, 5.3, 2.8, and $0.54 \mu\text{m}$, respectively. The curves d in Figs. 1(a) and 1(b) clearly show a shifted position for the Ga(In)As layer peak. Therefore, a simple peak separation measurement will result in a wrong lattice mismatch and layer composition.

In order to show the origin of shifting of the thin-layer peak, we briefly review the dynamical diffraction theory for a sample with a single epitaxial layer. The scattering amplitude X is defined as $D_H/D_0\sqrt{b}$, where D_H and D_0 are the diffracted and incident amplitudes, respectively, at the crystal surface. Scattering amplitude for a single epitaxial layer on a substrate is

$$\begin{aligned} X &= X_e + X_s, & X_e &= -iB \tan(sA)/Z, \\ X_s &= X_0[s - iC \tan(sA)]/Z, \\ Z &= [s + i(C + BX_0)\tan(sA)], \end{aligned} \quad (1)$$

where

$$B = -(1 + ik), \quad C = y + ig, \quad s = \sqrt{(C^2 - B^2)},$$

$$k = F''_H/F'_H, \quad g = -(1 + b)F''_0/(2F'_H\sqrt{b}),$$

$$b = |\gamma_0/\gamma_H|,$$

$$y = [-(1 + b)F'_0 + V(2\Delta\Theta \sin 2\Theta_B + C_1\epsilon_1)/$$

$$(\pi\lambda^2 r_e)]/(2F'_H\sqrt{b}),$$

$$C_1 = 2 \sin 2\Theta_B (\cos^2 \varphi \tan \Theta_B + \sin \varphi \cos \varphi),$$

$$A = \lambda r_e F'_H h / (V\sqrt{(|\gamma_0\gamma_H|)}),$$

$$\epsilon_1 = (1 + \nu)(a_f - a_s)/(1 - \nu)a_s,$$

h is layer thickness, λ is wavelength, r_e is electron radius, V is unit cell volume, γ_0 and γ_H are the direction cosines of incident and diffracted wave vectors relative to the inward surface-normal, $F'_{0,H}$ and $F''_{0,H}$ are the real and imaginary parts of the structure factor for incident (0) and diffracted waves (H), Θ_B is the Bragg angle, a_f and a_s are the layer and substrate lattice constants, and φ is the angle of inclination of the lattice plane with crystal surface. X_0 is the amplitude at the substrate-epilayer interface, which serves as the boundary condition for the dynamical x-ray diffraction from layered crystals. In Eq. (1), X_e is the epilayer amplitude and X_s is the substrate amplitude at the crystal surface.

Here, we must point out that much of the published literature^{5,8,9} quotes a wrong boundary condition, saying that the amplitude X is zero deep inside the substrate crystal. This is not true, because when the diffraction condition is met, D_H is zero only if D_0 is zero. The correct boundary condition is the amplitude at the layer-substrate interface, and this is the infinite-crystal solution to the Takagi-Taupin equation.¹⁰ This is^{3,11}

$$X_0 = -B/(C - s). \quad (2)$$

Now, the reflectivity is composed of three terms for a single-layer sample:

$$\text{Reflectivity} = |X|^2 = |X_e|^2 + |X_s|^2 + 2 \text{Re}(X_e^* X_s), \quad (3)$$

where Re denotes the real part of a complex quantity. Figure 2 shows the effect of the second term (overlap) and the third term (interference) to the position of the epilayer peak ($|X_e|^2$). It clearly demonstrates that the interference between the substrate and layer amplitudes is responsible for the layer peak shifting. Therefore, any approximation in diffraction theory, which gives an incorrect phase relationship between layer amplitude and substrate amplitude or which omits the interference term (as was done in Ref. 2 for the

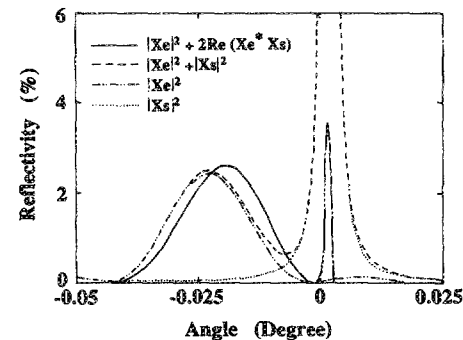


FIG. 2. Plot of various terms of Eq. (3) for a $0.25\text{-}\mu\text{m}$ $\text{Al}_{0.25}\text{Ga}_{0.75}\text{As}/\text{GaAs}(001)$. It shows that interference between the epilayer and substrate amplitudes is responsible for the epilayer peak shifting.

kinematical diffraction theory), will give an incorrect result for these thin-layer samples.

Figure 3(a) shows the epilayer peak position ($\Delta\theta$) with respect to the substrate peak position as a function of layer thickness, calculated from Eqs. (1)–(3). Here, $\Delta\theta$ is the actual peak separation and $\Delta\theta_0$ is when the overlap and interference effects are ignored. A 10% peak shifting occurs at 3000 Å for $\text{Al}_{0.25}\text{Ga}_{0.75}\text{As}/\text{GaAs}$, at 1500 Å for $\text{Al}_{0.5}\text{Ga}_{0.5}\text{As}/\text{GaAs}$ and $\text{Ga}_{0.476}\text{In}_{0.524}\text{As}/\text{InP}$, and at 800 Å for AlAs/GaAs . From this and from Eq. (1), which suggests that the peak shifting will depend on the product sh which is approximately proportional to $h\epsilon_l$, we plot in Fig. 3(b) the layer peak position as a function of $h\epsilon_l$ for various samples, reflection geometries, and wavelengths. Note that ϵ_l equals $(1 + \nu)/(1 - \nu)$ times the misfit ϵ_f . Figure 3(b) shows that the amount of peak shifting depends only the product of layer thickness and lattice misfit and is approximately independent of substrate, reflection geometry, and wavelength. For a 2% peak shifting, the layer thickness is given by

$$h = 3.9(1 - \nu)a_s / [(1 + \nu)(a_f - a_s)] \text{ \AA} \quad (4)$$

The layer lattice constant a_f may be estimated from Vegard's law using an approximate layer composition. Therefore, when the layer thickness is greater than the thickness given by Eq. (4), the simple peak separation method or the kinematical diffraction theory may be used. However, when it is

below, the dynamical diffraction theory should be used for analysis.

Finally, we show in Figs. 4(a) and 4(b) the simulated 004 $\text{CuK}\alpha_1$ rocking curves for 1.5- μm $\text{Al}_{0.5}\text{Ga}_{0.5}\text{As}/\text{Al}_x\text{Ga}_{1-x}\text{As}/1.5\text{-}\mu\text{m}$ $\text{Al}_{0.5}\text{Ga}_{0.5}\text{As}/\text{GaAs}$ (001) with $x = 0.35$ in Fig. 4(a) and $x = 0.15$ in Fig. 4(b). In both figures, the solid curve is for 0.4 μm , dashed curve for 0.5 μm , and dotted curve for 0.65 μm , respectively, for the sandwiched AlGaAs layer thickness. The sample is a double-heterojunction laser structure. Figure 4(a) shows that, when the thin-layer peak is closer to the thicker-layer peak in angular position, the thin-layer peak moves closer to the thicker-layer peak as its thickness decreases. However, when the thin-layer peak is closer to the substrate peak, there is little change in the peak position over the same thickness change, as Fig. 4(b) shows. Stronger influence by a thick layer on the thin-layer peak position than by the substrate is thought to be due to the fact that substrates do not produce diffraction fringes while the layers of finite thickness produce fringes that reach far in angle. Therefore, for multilayer samples, Eq. (4) can overestimate [as in Fig. 4(b)] or underestimate [as in Fig. 4(a)] the minimum thickness for use of the peak separation method. The diffraction fringes and interference structures (the small peaks and undulations in Fig. 4) are useful for characterization of heteroepitaxial samples including ultrathin (quantum well or quantum barrier) layers.^{12,13}

In summary, we showed that the peak separation method in rocking curve analysis must be used with care when the layer thickness and lattice mismatch are small. Equation (4)

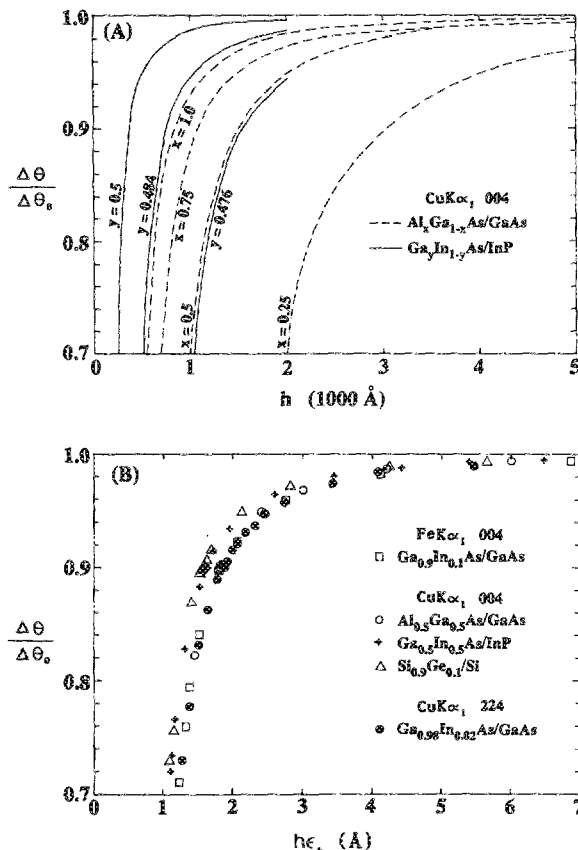


FIG. 3. (a) Plot of the separation between epilayer peak and substrate peak as a function of layer thickness. (b) Plot of the peak separation as a function of the product of thickness and perpendicular strain.

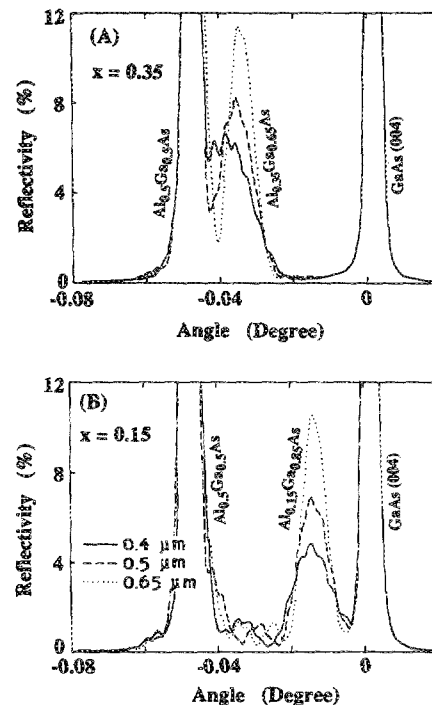


FIG. 4. Simulated rocking curves for 1.5- μm $\text{Al}_{0.5}\text{Ga}_{0.5}\text{As}/\text{Al}_x\text{Ga}_{1-x}\text{As}/1.5\text{-}\mu\text{m}$ $\text{Al}_{0.5}\text{Ga}_{0.5}\text{As}/\text{GaAs}$ (001) for $x =$ (a) 0.35 and (b) 0.15 at varying thickness of the $\text{Al}_x\text{Ga}_{1-x}\text{As}$ layer. The thicknesses are the same in (a) and (b).

gives the minimum layer thickness for a single layer sample. We demonstrated that the peak shifting is due to the interference between the thin-layer amplitude and other amplitudes. We point out that the boundary condition was incorrectly stated in many papers and that kinematical diffraction theory and the peak separation method have the same minimum thickness for the application range.

This work was supported by the National Science Foundation and by the Eastman Kodak Company.

- ¹E. Estop, A. Izrael, and M. Sauvage, *Acta Crystallogr. A* **32**, 627 (1976).
²V. S. Speriosu, *J. Appl. Phys.* **52**, 6094 (1981).

- ³C. R. Wie, T. A. Tombrello, and T. Vreeland, Jr., *J. Appl. Phys.* **59**, 3743 (1986).
⁴C. R. Wie, H. M. Kim, and K. M. Lau, *SPIE Proc.* **877**, 41 (1988).
⁵P. F. Fewster and C. J. Curling, *J. Appl. Phys.* **62**, 4154 (1987).
⁶J. F. Chen and C. R. Wie, *J. Electron. Mater.* **17**, 501 (1988), and references therein.
⁷J. F. Chen and C. R. Wie, *J. Electron. Mater.* (to be published).
⁸M. A. G. Halliwell, M. H. Lyons, and M. J. Hill, *J. Cryst. Growth* **68**, 523 (1984).
⁹J. Jeong, T. E. Schlesinger, and A. G. Milnes, *J. Cryst. Growth* **87**, 265 (1988).
¹⁰S. Takagi, *Acta Crystallogr.* **15**, 1311 (1962); D. Taupin, *Bull. Soc. Franc. Miner. Crystallogr.* **87**, 469 (1964).
¹¹C. R. Wie, Ph. D. Thesis, California Institute of Technology, 1985.
¹²C. R. Wie, (unpublished).
¹³C. R. Wie, *J. Appl. Phys.* **65**, 1036 (1989).

The influence of many-body effects on the gain and linewidth of semiconductor lasers

Witold Bardyszewski

Institute of Theoretical Physics, University of Warsaw, Hoza 69, 00 681 Warsaw, Poland

David Yevick

Department of Electrical Engineering, 121 Electrical Engineering East, Penn State University, University Park, Pennsylvania 16802 and Teoretisk Fysik, Lunds Universitet, Sölvegatan 14a, S-223 62 Lund, Sweden

(Received 30 November 1988; accepted for publication 20 March 1989)

We employ quantum-mechanical many-body theory to determine both the radiative recombination spectra and the linewidth broadening factor in III-V semiconductor diode lasers. We conclude correlation effects and the full $k \cdot p$ band structure in our calculation. Our results clearly illustrate the manner in which many-body effects relax momentum conservation in the recombination process.

Optical processes in solid-state light-emitting diodes and lasers have been the subject of intense theoretical analysis. Experimental results have generally been interpreted by assuming that the total momentum of the recombining electron-hole pair is not conserved in the recombination process in both doped and undoped semiconductors.^{1,2} While theoretical models have been constructed which are solely based on changes in the density of states and the degree of k conservation at the band extrema associated with local fluctuations in the electron and hole densities,^{3,4} most work has centered on the role of many-body effects. Unfortunately, the interference term in the gain in the lowest-order approximation with respect to the electron-plasmon coupling is divergent for $\hbar\omega = E_g$.^{5,6} In a somewhat heuristic model this divergence has been avoided by broadening the electron propagators;⁷ however, most researchers have approximated the electron-electron interaction and the band structure in order to sum the ladder diagrams for the interband polarization function.⁸⁻¹⁰ A divergenceless theory is also generated by neglecting correlation effects, although this produces an unrealistic broadening of the gain curve. While occasionally cited as an explanation of band tailing,¹¹ this effect is generally eliminated by neglecting the interaction of electrons with plasmons¹² or by selecting a value of the $T = 300$ K GaAs electron lifetime τ on the order of 0.5 ps.¹³ Such values, however, conflict with recent results which indicate that

$\tau \cong 0.03$ ps.¹⁴ Further, since the matrix elements in these calculations are momentum-conserving, the gain curves do not display the features of k nonconservation.

In this communication, we evaluate the gain spectrum using realistic expressions for the spectral density functions, overlap matrix elements, and correlation effects associated with virtual and real plasmon emission by the recombining electron-hole pair. A series of approximations then leads to a simple and rapid algorithm for the gain profile which is free of band-edge singularities.

Beside the optical gain, another quantity of great experimental interest is the dependence of the real and imaginary refractive index components on carrier density. Theoretical studies here have considered momentum-conserving recombination between electrons and holes with Lorentzian spectral density functions.^{12,13} The results are relatively insensitive to the particle lifetimes and therefore agree qualitatively with experiment.

Our first objective in this study is to calculate the optical gain, defined in terms of the conductivity by $g(\omega) = -4\pi \text{Re } \sigma(\omega)/cn_r$. The conductivity in turn may be written as a sum of the products of Coulomb matrix elements with the components of the retarded linear response function. Suppressing band indices, integration symbols, and coordinate and time variables, we can express the linear response function as $L = -i\hbar[G G + G(\delta\Sigma/\delta U)G]$. Con-